THE JOURNAL OF BIOLOGICAL CHEMISTRY VOL. 283, NO. 16, pp. 10522–10534, April 18, 2008

Targeted Depletion of Hepatic ACAT2-driven Cholesterol Esterification Reveals a Non-biliary Route for Fecal Neutral Sterol Loss*

Received for publication, September 12, 2007, and in revised form, February 14, 2008 Published, JBC Papers in Press, February 14, 2008, DOI 10.1074/jbc.M707659200

J. Mark Brown[‡], Thomas A. Bell III[§], Heather M. Alger[¶], Janet K. Sawyer[‡], Thomas L. Smith[‖], Kathryn Kelley[‡], Ramesh Shah[‡], Martha D. Wilson[‡], Matthew A. Davis[‡], Richard G. Lee[**], Mark J. Graham[**], Rosanne M. Crooke[**], and Lawrence L. Rudel[‡¶1]

From the Departments of [‡]Pathology, [¶]Biochemistry, and [‖]Orthopedic Surgery, Wake Forest University School of Medicine, Winston-Salem, North Carolina 27157-1040, the [§]Department of Immunology, The Scripps Research Institute, La Jolla, California 92037, and the [**]Cardiovascular Group, Antisense Drug Discovery, Isis Pharmaceuticals, Inc., Carlsbad, California 92008-7208

Deletion of acyl-CoA:cholesterol *O*-acyltransferase 2 (ACAT2) in mice results in resistance to diet-induced hypercholesterolemia and protection against atherosclerosis. Recently, our group has shown that liver-specific inhibition of ACAT2 via antisense oligonucleotide (ASO)-mediated targeting likewise limits atherosclerosis. However, whether this atheroprotective effect was mediated by: 1) prevention of packaging of cholesterol into apoB-containing lipoproteins, 2) augmentation of nascent HDL cholesterol secretion, or 3) increased hepatobiliary sterol secretion was not examined. Therefore, the purpose of these studies was to determine whether hepatic ACAT2 is rate-limiting in all three of these important routes of cholesterol homeostasis. Liver-specific depletion of ACAT2 resulted in reduced packaging of cholesterol into apoB-containing lipoproteins (very low density lipoprotein, intermediate density lipoprotein, and low density lipoprotein), whereas high density lipoprotein cholesterol levels remained unchanged. In the liver of ACAT2 ASO-treated mice, cholesterol ester accumulation was dramatically reduced, yet there was no reciprocal accumulation of unesterified cholesterol. Paradoxically, ASO-mediated depletion of hepatic ACAT2 promoted fecal neutral sterol excretion without altering biliary sterol secretion. Interestingly, during isolated liver perfusion, ACAT2 ASO-treated livers had augmented secretion rates of unesterified cholesterol and phospholipid. Furthermore, we demonstrate that liver-derived cholesterol from ACAT2 ASO-treated mice is preferentially delivered to the proximal small intestine as a precursor to fecal excretion. Collectively, these studies provide the first insight into the hepatic itinerary of cholesterol when cholesterol esterification is inhibited only in the liver, and provide evidence for a novel non-biliary route of fecal sterol loss.

The central role of the liver in regulating both the production and clearance of circulating lipoprotein cholesterol is well recognized (reviewed in Refs. 1–4). However, hepatic cholesterol homeostasis is articulated through the interplay of many distinct pathways including *de novo* synthesis, delivery of dietary cholesterol from the intestine, biliary secretion, and secretion in nascent lipoproteins (1–5). It has been demonstrated that the majority of cholesterol absorbed by the intestine is directed into the liver (5), where it not only affects *de novo* cholesterol synthesis, but also regulates cholesterol esterification and packaging into nascent lipoproteins (1–5). Hence, when the amount of dietary cholesterol delivered by chylomicron remnants is low, *de novo* cholesterol synthesis is increased. In this case the liver uses this pool of cholesterol for normal functions such as membrane biogenesis, lipoprotein synthesis, and bile acid synthesis. However, when dietary cholesterol absorption is high the liver pool is expanded, resulting in reduction of *de novo* synthesis, and increased secretion of cholesterol in apoB-containing lipoproteins. Atherosclerosis can eventually result if these apoB-containing lipoproteins remain in the circulation for extended periods at high concentrations. Therefore, factors influencing intestinal absorption, chylomicron packaging, and hepatic retention of cholesterol are crucial in controlling hypercholesterolemia and atherosclerosis.

Cholesterol esterification is intimately involved in all of these processes, and it is now appreciated that three distinct enzymes catalyze this reaction. Lecithin-cholesterol acyltransferase (LCAT)[2] acts exclusively in the plasma to esterify lipoprotein-associated cholesterol, whereas acyl-CoA:cholesterol *O*-acyltransferases 1 (ACAT1) and 2 (ACAT2) are intracellular enzymes with distinct tissue distributions and functions (6–10). ACAT1 is ubiquitously expressed in almost all non-lipoprotein producing cell types, and acts to prevent free cholesterol-induced cytotoxicity (reviewed in Ref. 6). On the other hand ACAT2 is expressed exclusively in lipoprotein-producing

* This work was supported by National Institutes of Health Grants P01-HL49373 (to L. L. R.) and T32 HL07115-28 (to J. M. B.) and American Heart Association postdoctoral fellowship 0625400U (to J. M. B.). The costs of publication of this article were defrayed in part by the payment of page charges. This article must therefore be hereby marked "*advertisement*" in accordance with 18 U.S.C. Section 1734 solely to indicate this fact.

[1] To whom correspondence should be addressed: Dept. of Pathology, Section on Lipid Sciences, Wake Forest University School of Medicine, Medical Center Blvd., Winston-Salem, NC 27157-1040. Tel.: 336-716-2821; Fax: 336-716-6279; E-mail: lrudel@wfubmc.edu.

[2] The abbreviations used are: LCAT, lecithin-cholesterol acyltransferase; ABCA1, ATP-binding cassette transporter A1; ACAT2, acyl-coenzyme A:cholesterol acyltransferase 2; CE, cholesteryl ester; Cyp7α1, cholesterol 7α-hydroxylase; FC, free cholesterol; HDL, high density lipoprotein; LDL, low density lipoprotein; LXR, liver X receptor; PL, phospholipid; SHP, small heterodimeric partner; TC, total cholesterol; TG, triglyceride; VLDL, very low density lipoprotein; SI, small intestine; ASO, antisense oligonucleotide.

cells such as intestinal enterocytes and hepatocytes in the liver (7, 8), and plays a gatekeeper role in the production of atherogenic apoB-containing lipoproteins (6–10). In support of this concept, when compared with wild type controls, ACAT2-deficient mice have reduced cholesterol absorption (11–14), are depleted in hepatic cholesteryl esters (CE) (7–14), and are protected against diet-induced gallstone formation and atherosclerosis (10, 11, 15). Importantly, the hepatic storage and secretion of CE into apoB-containing lipoproteins is virtually absent in mice lacking ACAT2 (9–14), indicating that ACAT2 is the sole cholesterol-esterifying enzyme in mouse liver. Collectively, these data point toward ACAT2 as a crucial regulator of both intestinal and hepatic cholesterol metabolism and ultimately atherosclerosis. However, the original total body model of ACAT2 deficiency (11) has left many unanswered questions regarding the relative importance of intestinal ACAT2 in promoting cholesterol absorption *versus* the role of hepatic ACAT2 in the packaging of CE into atherogenic apoB-containing lipoproteins.

To specifically address the role of ACAT2 in hepatic cholesterol metabolism we have successfully created an *in vivo* antisense oligonucleotide (ASO) liver targeting system (14). Using this system, hepatic ACAT2 expression is depleted, whereas intestinal ACAT2 expression and intestinal cholesterol absorption is left undisturbed, thereby maintaining essentially normal amounts of intestinally absorbed cholesterol to the liver. Using this strategy we have previously demonstrated that liver-specific depletion of ACAT2 limits diet-induced hypercholesterolemia and atherosclerosis (14). However, whether this atheroprotective effect was mediated by: 1) prevention of packaging of cholesterol into apoB-containing lipoproteins, 2) augmentation of nascent HDL cholesterol secretion, or 3) increased hepatobiliary sterol secretion was not examined. Therefore, using *in vivo* ASO-mediated reduction of hepatic ACAT2, the current study was undertaken to address the following question: under a moderate dietary cholesterol burden, what is the fate of hepatic cholesterol when it cannot be esterified?

We originally suspected that targeted depletion of ACAT2-driven hepatic cholesterol esterification would prevent secretion of CE in atherogenic apoB-containing lipoproteins into the plasma compartment, potentially augment HDL cholesterol levels, and stimulate the hepatobiliary secretion of cholesterol. Results from this study indicate that indeed liver-specific depletion of ACAT2 resulted in reduced packaging of CE into apoB-containing lipoproteins, yet had no effect on HDL cholesterol levels. Parodoxically, liver-specific depletion of ACAT2 resulted in increased fecal sterol loss without changes in biliary sterol excretion. This led us to examine the possibility of a novel non-biliary pathway (liver → plasma → small intestine → feces) for moving cholesterol out to the proximal small intestine when hepatic cholesterol esterification is compromised.

EXPERIMENTAL PROCEDURES

Animals—Male apoB100-only, LDLr$^{-/-}$ mice harboring homozygous wild type (ACAT2$^{+/+}$) or knock-out (ACAT2$^{-/-}$) ACAT2 alleles were bred as previously described (16). All mice were on a mixed background (~50% C57BL/6 and ~50% 129Sv/Jae). Therefore, sibling controls were used and assignment to treatment groups was randomized to minimize effects of genetic heterogeneity. At 6 weeks of age, the mice were switched from a diet of rodent chow to a low fat (20% of energy as palm oil-enriched fat) and moderate cholesterol (0.1%, w/w), and randomly assigned to one of three treatment groups. During the eight-week dietary regimen, mice were injected biweekly either saline, 25 mg/kg of a non-targeting ASO (control ASO; 5′-GTCGCTCAACATCTGAATCC-3′), or 25 mg/kg of an ASO targeting the knockdown of ACAT2 (ACAT2 ASO; 5′-TTCGGAAATGTTGCACCTCC-3′) as previously described (14). The ACAT2 ASO used in the current study corresponds to ASO 6 from our previous report (14). Data shown are from mice that had undergone 8 weeks of parallel ASO treatment and dietary induction, except for a subset of 8 mice used specifically for liver perfusion experiments that were treated for 14–16 weeks to maximize knockdown (see Fig. 6*C*). All mice were maintained in an American Association for Accreditation of Laboratory Animal Care-approved animal facility, and all experimental protocols were approved by the institutional animal care and use committee at the Wake Forest University School of Medicine.

Plasma Lipid and Lipoprotein Analyses—Total plasma cholesterol and plasma triglyceride (TG) concentrations were measured using colorimetric assay as previously described (9, 10, 13, 14, 16). Cholesterol concentrations in very low density lipoproteins (VLDL), intermediate density lipoproteins, low density lipoproteins (LDL), and high density lipoproteins (HDL) were determined after separation of pooled plasma (n = 5 per group) by high pressure liquid chromatography with a GE Healthcare Superose-6 column run at a flow rate of 0.5 ml/min, as previously described (10). For whole plasma immunoblotting, 1 μl of plasma was diluted 1000 times with a modified RIPA buffer containing phosphate-buffered saline (pH 7.5), 1% Nonidet P-40, 0.1% SDS, 0.5% sodium deoxycholate, 500 μM 4-(2-aminoethyl)benzenesulfonyl fluoride, 1 μg/ml aprotinin, 1 μM E-64, 500 μM EDTA, and 1 μM leupeptin. Ten μl of diluted plasma was separated by 4–12% gradient SDS-PAGE, and immunoblotted with the following antibodies: 1) goat anti-human apoB IgG (Academy Biomedical Co.), 2) rabbit anti-rat apoE serum (kindly provided by J. Herz, University of Texas Southwestern Medical Center, Dallas, TX), 3) rabbit anti-human apoA-I IgG (Biodesign), or 4) rabbit anti-mouse LCAT serum (kindly provided by J. S. Parks, Wake Forest University School of Medicine, Winston-Salem, NC).

Immunoblotting of Hepatic and Intestinal Proteins—Total liver homogenates were made in a modified RIPA buffer containing phosphate-buffered saline (pH 7.5), 1% Nonidet P-40, 0.1% SDS, 0.5% sodium deoxycholate, 2 mM Na_3VO_4, 20 mM β-glycerophosphate, 10 mM sodium fluoride, and a protease inhibitor mixture (Calbiochem) including 500 μM 4-(2-aminoethyl)benzenesulfonyl fluoride, 1 μg/ml aprotinin, 1 μM E-64, 500 μM EDTA, and 1 μM leupeptin. Homogenates (25 μg/lane) were separated by 4–12% SDS-PAGE, transferred to polyvinylidene difluoride membrane, and incubated with the following antibodies: 1) rabbit anti-African green monkey ACAT2 IgG (8), 2) rabbit anti-mouse ABCA1 serum (kindly provided by J. S. Parks, Wake Forest University), 3) mouse monoclonal Akt1 (2H10) IgG (Cell Signaling Technologies, Inc., number 2967),

4) chicken polyclonal Cyp7α-hydroxylase IgY (18), and 5) rabbit polyclonal antipeptide antibody against SR-BI (Q820-6, kindly provided by Helen Hobbs, University of Texas Southwestern Medical Center).

Quantitative Real-time PCR—RNA extraction and quantitative PCR was conducted as previously described (13) on pooled samples ($n = 5$ per group). Cyclophilin was used as an internal control for these studies, and the cycle number of cyclophilin was subtracted from the cycle number of each gene in the same sample. The values of mRNA levels for each gene represent the amount relative to the amount in the saline-treated group, which was arbitrarily standardized to 100%. Primers used for quantitative PCR are as follows: ACAT2: forward, 5′-GACTTGGTGCAATGGACTCG-3′, reverse, 5′-GGTCTTGCTTGTAGAATCTGG-3′; ATP binding cassette transporter A1 (ABCA1): forward, 5′-CGTTTCCGGGAAGTGTCCTA-3′, reverse, 5′-GCTAGAGATGACAAGGAGGATGGA-3′; ATP binding cassette transporter G5 (ABCG5): forward, 5′-GGCAGGTTTTCTCGATGAACTG-3′, reverse, 5′-ATTTTTAAAGGAATGGGCATCTCTT-3′; 3-hydroxy-3-methylglutaryl-CoA synthase 1: forward, 5′-GCCGTGAACTGGGTCGAA-3′, reverse, 5′-GCATATATAGCAATGTCTCCTGCAA-3′; cholesterol 7α hydroxylase (Cyp7α1): forward, 5′-AGCAACTAAACAACCTGCCAGTACTA-3′, reverse, 5′-GTCCGGATATTCAAGGATGCA-3′; cyclophilin: forward, 5′-TGGAGAGCACCAAGACAGACA-3′, reverse, 5′-TGCCGGAGTCGACAATGAT-3′.

Microsomal ACAT Assay—Liver microsomes were prepared and *in vitro* ACAT activity assays were performed as previously described (7, 19).

Cholesterol Absorption and Fecal Neutral Sterol Excretion Measurements—Fractional cholesterol absorption was measured using the fecal dual isotope method, and fecal neutral sterol excretion was measured by gas-liquid chromatography as previously described (13).

Biliary Lipid Collection and Analysis—Determination of lipid concentrations in gall bladder bile lipid was conducted as previously described (13). For measurement of lipid concentrations in newly secreted bile, common bile duct cannulations were performed as previously described (17).

Tissue Lipid Mass Determination—Tissue lipid extracts were made and total cholesterol (TC), cholesterol ester (CE), free cholesterol (FC), triglyceride (TG), or phospholipid (PL) mass was measured using enzymatic assays as previously (10, 13–14).

Determination of Hepatic Lipid Secretion by Isolated Liver Perfusion—Isolated recirculating liver perfusions were performed using chemically defined plasma-free medium as described previously (9, 20). Two separate sets of experimental mice (acute *versus* chronic treatment) were studied. The first set of mice was treated for 8 weeks with ASOs (data represented in Fig. 4*A*), and accumulation rates were determined using enzymatic assays as previously described (9, 20) with minor modifications. Because ACAT2 ASO-treated mice had significantly larger liver weights (6.1% of body weight), when compared with all other groups (4.67% in control ASO-treated mice and 4.02% in saline treated ACAT2$^{-/-}$ mice), lipid accumulation rate data are expressed as micrograms/ml/liver, and were not normalized to liver weight as previously described (9). The second set of mice used for liver perfusion was treated more chronically (14–16 weeks) in an attempt to completely deplete the hepatic ACAT2 activity. In this set of mice liver perfusions were conducted as described above, but all sterol mass accumulation rates were determined by gas-liquid chromatography instead of enzymatic assays.

Quantification of Non-biliary (Liver → Plasma → Intestine → Feces) Fecal Cholesterol Loss—All mice used for this protocol were treated for a period of 12–16 weeks with either a control (non-targeting) ASO or an ASO targeting the knockdown of ACAT2. Thereafter, hepatic sterol pools were radiolabeled in a subset of donor mice ($n = 3$ per group) by gavaging 50 μCi of [1,2-^{3}H]cholesterol (PerkinElmer Life Sciences) in 100 μl of soybean oil vehicle just prior to the dark cycle. Twelve hours post-gavage, mice were anesthetized with 15 mg/kg ketamine and 1.5 mg/kg xylazine, and recirculating isolated liver perfusions were carried out as previously described (9) to collect nascent liver-derived lipoproteins containing [^{3}H]cholesterol. The final perfusate time point (roughly 7.5 ml) was concentrated down to ~400 μl using a Centricon YM-30 concentrator (30,000 molecular weight cut-off; Millipore). Greater than 99% of lipoprotein-associated [^{3}H]cholesterol was recovered in the upper chamber following centrifugation. The concentrated liver perfusate samples were delivered (injections ranged from $\sim 1.5 \times 10^5$ to 3.7×10^5 dpm of [^{3}H]cholesterol) into the circulation of isoflurane (4% induction, 2% maintenance) anesthetized recipient mice by jugular vein injection. Recipient mice regained consciousness within 5 min of isoflurane withdrawal, and were housed with *ad libitum* access to food and water for 6 h. Thereafter, recipient mice were anesthetized with 15 mg/kg ketamine and 1.5 mg/kg xylazine for subsequent tissue collection. Following gall bladder bile and plasma collection, a whole body flush was conducted by puncturing the inferior vena cava and slowly delivering 10 ml of saline into the heart to clear plasma lipoprotein-associated [^{3}H]cholesterol from tissues. Thereafter, the liver and small intestine (SI) were removed for subsequent analysis. The intestine was divided into four equal segments that were classified proximal to distal as SI-1, SI-2, SI-3, and SI-4. All SI segments were gently washed twice with 2 ml of saline to collect intestinal lumenal contents, and the remaining intestine was blotted dry and subsequently analyzed. All tissues and lumenal contents were extracted by the method of Bligh and Dyer (21), and an aliquot of the organic phase was dried down under nitrogen subsequently analyzed by scintillation counting. All data are expressed as the percent of the total dose injected into each recipient mouse (dpm in tissue/dpm in dose × 100).

Statistical Analyses—Data are expressed as the mean ± S.E. All data were analyzed using one-way analysis of variance followed by Student's t tests for post hoc analysis. Differences were considered significant at $p < 0.05$. All analyses were performed using JMP version 5.0.12 (SAS Institute. Cary, NC) software.

RESULTS

ASO-mediated Knockdown of ACAT2 Occurs in a Liver-specific Manner—To determine the tissue specificity of ASO-mediated knockdown of ACAT2, we examined mRNA expression, protein expression, and function of ACAT2 in the only two

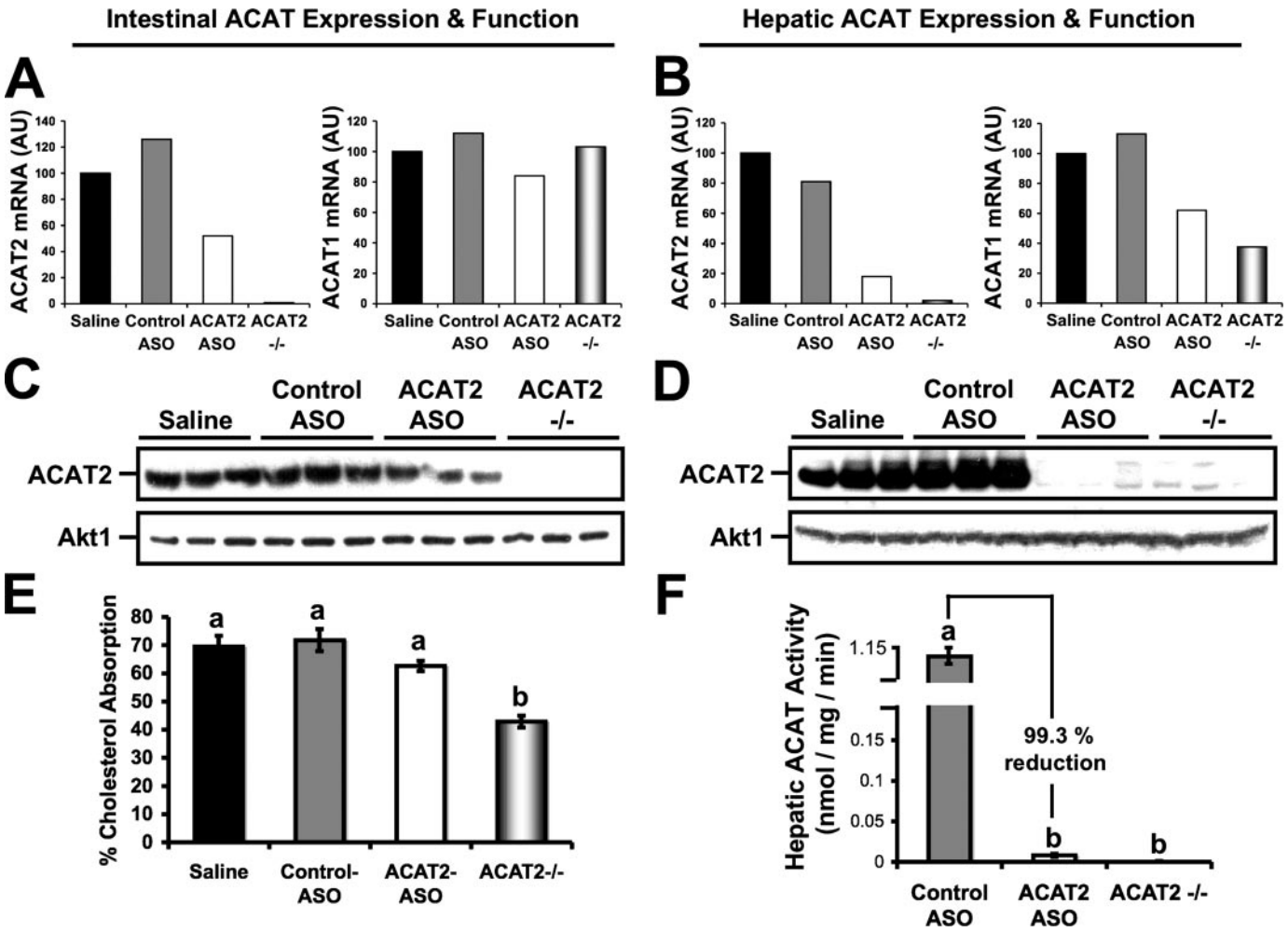

FIGURE 1. **ASO-mediated knockdown of ACAT2 is liver-specific.** Male LDLr$^{-/-}$, apoB100-only mice were fed a low-fat (20% of energy as fat), moderate cholesterol (0.1%, w/w) diet for 8 weeks in conjunction with biweekly injections (25 mg/kg) of saline, a non-targeting ASO (*control ASO*), or an ASO targeting the knockdown of ACAT2 (*ACAT2 ASO*). Mice with targeted gene deletion of ACAT2 were treated with saline as a total body knock-out control (*ACAT2*$^{-/-}$). Relative quantitation of ACAT1 and ACAT2 mRNA transcripts in proximal small intestine (*A*) or liver (*B*) was conducted by real-time PCR as described under "Experimental Procedures." Data shown in *panels A* and *B* represent pooled RNA samples with $n = 5$ mice per group. *Panels C* and *D* represent Western blot analysis of ACAT2 and Akt1 protein expression in proximal small intestine (*C*) or liver (*D*) homogenates ($n = 3$ per group). *Panel E* represents fractional cholesterol absorption measured by the fecal dual-isotope method. Data in *panel E* represent the mean ± S.E. from seven to nine mice per group, and values not sharing a common superscript differ significantly ($p < 0.05$). *Panel F* represents hepatic ACAT activity of cholesterol pre-loaded liver microsomes. Data in *panel F* represent the mean ± S.E. from four to five mice per group, and values not sharing a common superscript differ significantly ($p < 0.05$).

tissues that ACAT2 is known to be expressed (7, 8), the small intestine and liver. After 8 weeks of treatment, there was a striking reduction in hepatic ACAT2 mRNA (Fig. 1*B*), protein (Fig. 1*D*), and microsomal ACAT activity (Fig. 1*F*) in mice treated with the ACAT2 ASO, compared with saline or control ASO-treated mice. In fact, the residual ACAT activity seen in ACAT2 ASO-treated livers was only 0.7% of that seen in control ASO-treated livers (Fig. 1*F*). In contrast to effects seen in the liver, the proximal third of the small intestine demonstrated a ~40–50% reduction in ACAT2 mRNA (Fig. 1*A*), protein (Fig. 1*C*), yet no significant reduction in fractional cholesterol absorption (Fig. 1*E*) by ACAT2 ASO treatment. This result indicates that even though ACAT2 ASO treatment reduced intestinal ACAT2 mRNA protein expression by ~40–50%, there was still enough functional ACAT2 protein to facilitate typical amounts of cholesterol absorption. This tissue-specific pattern of inhibition likely has to due with the well documented tissue distribution of phosphorothioate ASOs (22). The tissue-specific nature of ASOs was important because we wanted to create a situation where the liver would be subjected to a normal burden of intestinally derived cholesterol, yet would not be able to esterify cholesterol locally in the liver.

Furthermore, we examined the unlikely possibility that ACAT1 mRNA abundance could be altered by ACAT2 ASO treatment. In the proximal small intestine, ACAT1 mRNA abundance was similar in all treatment groups (Fig. 1*A*), supporting target specificity for the ACAT2 ASO. Interestingly, in the livers of ACAT2 ASO-treated and ACAT2$^{-/-}$ mice we found reduced abundance of ACAT1 mRNA (Fig. 1*B*), when compared with saline or control ASO-treated mice. We believe that this effect may be due to decreased macrophage content in livers of ACAT2 ASO-treated and ACAT2$^{-/-}$ mice, because cd68 mRNA abundance was decreased to a similar extent in these livers (data not shown).

ASO-mediated Knockdown of ACAT2 Reduces Cholesterol Packaging into ApoB-containing Lipoproteins, Without Affect-

ing HDL Cholesterol Levels—We have previously demonstrated that liver-specific depletion of ACAT2 limits diet-induced hypercholesterolemia and atherosclerosis following a 16-week chronic ASO treatment regimen (14). However, after 16 weeks of diet and ASO treatment, we saw nonsignificant effects on VLDL and LDL cholesterol levels when comparing mice treated with saline to the ACAT2 ASO used in the current study (ASO 6 from previous paper) (14). In line with this, we hypothesized that more robust differences could be observed after only 8 weeks of treatment, potentially explaining the previously observed atheroprotection seen with ASO 6 (14). As seen in Fig. 2, after 8 weeks of ACAT2 ASO treatment, total plasma cholesterol (Fig. 2*A*), VLDL cholesterol (Fig. 2*B*), and LDL cholesterol (Fig. 2*C*) were all reduced by ~50% when compared with control ASO-treated mice, and were similar to levels seen in whole body ACAT2 knock-out mice. In contrast, HDL cholesterol levels were similar in all treatment groups (Fig. 2*D*), indicating that when hepatic cholesterol esterification is limited (*i.e.* ACAT2 ASO treatment), the resulting free cholesterol burden is not likely shunted to HDL biogenesis via ABCA1-mediated efflux.

As has been previously reported (10–11, 13–16), plasma triglyceride levels were elevated in ACAT2 ASO-treated and ACAT2$^{-/-}$ mice, when compared with control ASO-treated and saline-treated groups (Fig. 2*E*). This ACAT2 depletion-induced hypertriglyceridemia is a highly reproducible effect in all studies done to date that occurs by an unidentified mechanism. When cholesterol distribution across lipoprotein particles was determined by size exclusion chromatograpy, we observed normal VLDL, LDL, and HDL sized particles, with no detectable aberrant lipoprotein particle sizes in any treatment group (Fig. 2*F*). Furthermore, when the mass of apolipoproteins A-I, E, and B in whole plasma was examined there were no obvious abnormalities in any of the treatment groups (Fig. 2*G*). In addition, abundance of the plasma cholesterol esterifying enzyme LCAT was similar in all treatment groups (Fig. 2*G*).

ASO-mediated Depletion of ACAT2 Strongly Reduces Hepatic Cholesterol Esterification, Yet Does Not Cause Free Cholesterol Accumulation in the Liver—Given that ACAT2 ASO treatment resulted in a 99.3% reduction in hepatic ACAT2 protein and activity (Fig. 1, *D* and *F*), we anticipated that hepatic cholesterol ester mass would be diminished. Furthermore, we expected that hepatic free cholesterol could build up with ACAT2 ASO treatment, unless compensatory mechanisms acted to remove the excess free cholesterol burden. Indeed, when compared with mice treated with control ASO, mice treated with the ACAT2 ASO had a 50% reduction in hepatic total cholesterol (Fig. 3*A*), a result of the reduction in hepatic cholesteryl ester (Fig. 3*B*). Strikingly, even in the face of a 71% reduction in hepatic cholesteryl ester mass, ACAT2 ASO-treated livers did not accumulate free cholesterol when compared with control ASO-treated livers (Fig. 3*C*). In fact ACAT2$^{-/-}$ mice had significantly less free cholesterol compared with all other groups, despite a complete lack of hepatic cholesterol esterification (Fig. 3*C*). Hepatic phospholipid content was similar in all treatment groups, with ACAT2$^{-/-}$ mice having the lowest levels (Fig. 3*D*).

The liver has several mechanisms that coordinate cholesterol homeostasis to prevent the accumulation of cytotoxic amounts of free cholesterol (1–5). It is well known that sterol-sensing transcription factors such as the sterol response element-binding proteins (SREBP) and the liver X receptors (LXRs) orchestrate *de novo* cholesterol synthesis and sterol efflux pathways, respectively, to maintain hepatic sterol homeostasis (1–5). Therefore, we examined the mRNA abundance of known target genes of both of these sterol-sensing transcription factors. As seen in Fig. 4*A*, the mRNA abundance of ABCA1, ABCG5, and 3-hydroxy-3-methylglutaryl-CoA synthase were not dramatically different between any of the treatment groups. Furthermore, the mRNA abundance of the rate-limiting enzyme in bile acid synthesis, Cyp7α1, was not dramatically altered by any treatment (Fig. 4*A*). We also examined the protein expression of several key proteins known to regulate hepatic sterol flux, and found that only ABCA1 was modulated by ACAT2 ASO treatment. To this end, hepatic ABCA1 protein expression was modestly increased in ACAT2 ASO-treated mice when compared with all other groups, whereas Cyp7α1, and scavenger receptor BI protein expression was not altered by any treatment (Fig. 4*B*). The modest up-regulation of ABCA1 protein (Fig. 4*B*), without corresponding alteration in ABCA1 (Fig. 4*A*) seen in ACAT2 ASO-treated livers may indicate post-transcriptional regulation.

ASO-mediated Depletion of Hepatic Cholesterol Esterification Does Not Result in Cholesterol Accumulation in Extrahepatic Tissues—The fact that liver-specific depletion of ACAT2 resulted in dramatic reductions in hepatic CE storage (Fig. 3*B*) without reciprocal increases in hepatic free cholesterol (Fig. 3*C*) led us to postulate that excess unesterified cholesterol could be transferred to extrahepatic tissues for storage purposes. In agreement with previous results (Ref. 14 and Fig. 3), treatment with the ACAT2 ASO resulted in a 64% reduction in hepatic cholesterol levels (Fig. 5), yet there was no obvious compensatory storage of cholesterol in extrahepatic tissues (Fig. 5). In fact, ACAT2 ASO treatment resulted in a significant 24% reduction in the cholesterol concentration in spleen and an apparently large (37%) although nonsignificant reduction in average adrenal cholesterol concentration (Fig. 5). In addition, there was a small (9%) but significant reduction in kidney cholesterol levels with ACAT2 ASO treatment (Fig. 5). For all other tissues, treatment with the ACAT2 ASO did not result in significant alterations in cholesterol mass. These data suggest that liver-specific depletion of ACAT2 results in not only the loss of hepatic cholesterol storage (Figs. 3 and 5), but also modest reductions in spleen, adrenal, and kidney cholesterol (Fig. 5). This is an important observation because we know that ACAT2 ASO-treated mice readily absorb cholesterol through the intestine (Fig. 1*E*) (14), yet the dietary cholesterol burden does not result in extrahepatic tissue accumulation of cholesterol.

Depletion of ACAT2 Results in Abundant Cholesteryl Ester and Augmented Free Cholesterol Secretion from the Liver—Given that ACAT2 ASO treatment resulted in a 99.3% reduction in hepatic ACAT2 protein and activity (Fig. 1, *D* and *F*), with a concomitant reduction in hepatic CE mass by 71% (Fig. 3*B*), we anticipated that packaging of hepatic CE into apoB-containing VLDL particles would be likewise dramatically

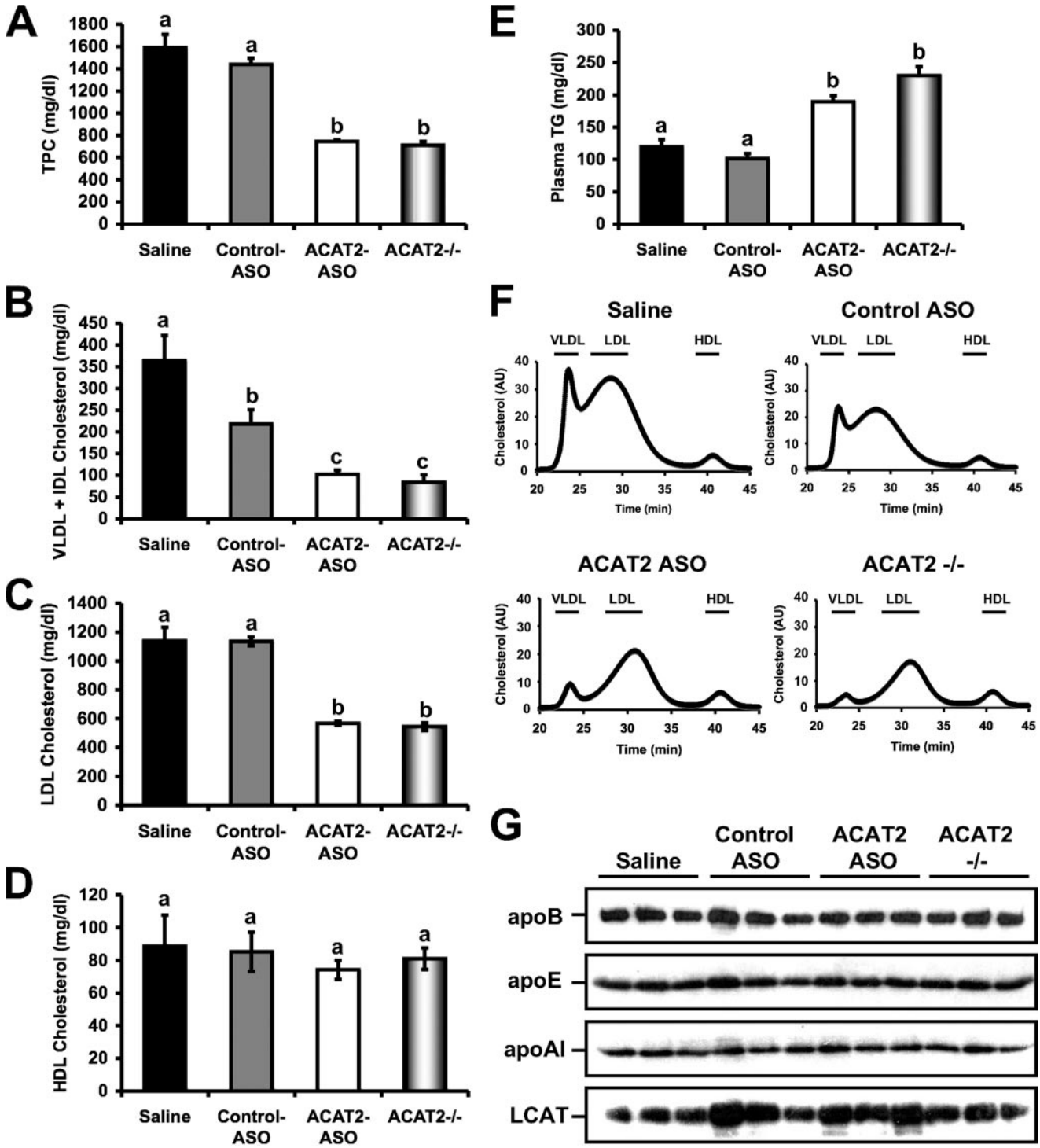

FIGURE 2. **ASO-mediated knockdown of ACAT2 reduces cholesterol packaging into apoB-containing lipoproteins, without affecting HDL cholesterol levels.** Male LDLr$^{-/-}$, apoB100-only mice were fed a low-fat (20% of energy as fat), moderate cholesterol (0.1%, w/w) diet for 8 weeks in conjunction with biweekly injections (25 mg/kg) of saline, a non-targeting ASO (*control ASO*), or an ASO targeting the knockdown of ACAT2 (*ACAT2 ASO*). Mice with targeted gene deletion of ACAT2 were treated with saline as a total body knock-out control (*ACAT2*$^{-/-}$). Fasting plasma samples were separated by size exclusion chromatography and enzymatically analyzed to quantify: *A*, total plasma cholesterol; *B*, very low density lipoprotein and intermediate-density lipoprotein cholesterol (*VLDL + IDL*); *C*, LDL cholesterol; *D*, HDL cholesterol; and *E*, whole plasma TG. *Panel F* represents the cholesterol distribution of plasma lipoprotein fractions determined by size exclusion chromatography coupled to online cholesterol analysis, where 30 μl of pooled plasma ($n = 5$ per group) was applied to a FPLC Superose 6 column and cholesterol concentration is expressed in arbitrary units (*AU*). *Panel G* represents quantification of whole plasma apolipoprotein B (*apoB*), apolipoprotein E (*apoE*), apolipoprotein A-I (*apoA-I*), and LCAT levels by Western blotting ($n = 3$ per group). Data represented in *panels A–E* represent the mean ± S.E. from seven to nine mice per group, and values not sharing a common superscript differ significantly ($p < 0.05$).

reduced. Paradoxically, during isolated liver perfusion experiments, the secretion rate of hepatic CE was similar in control ASO-treated mice and ACAT2 ASO-treated mice after 8 weeks of treatment (Fig. 6*A*). In contrast, the secretion rate of hepatic CE was virtually absent in ACAT2$^{-/-}$ mice (Fig. 6*A*), which is in agreement with previous reports (9). Interestingly during

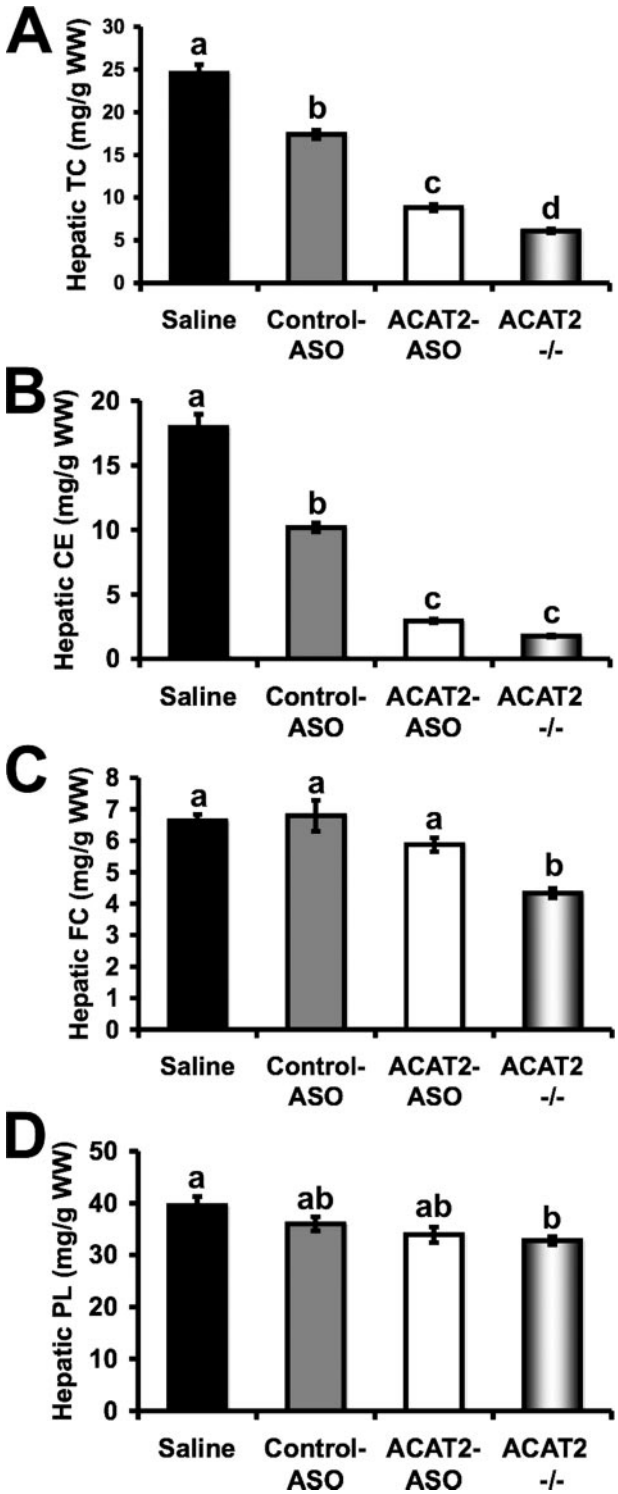

FIGURE 3. **ASO-mediated depletion of ACAT2 reduces hepatic cholesterol esterification, yet does not cause free cholesterol accumulation in the liver.** Male LDLr$^{-/-}$, apoB100-only mice were fed a low-fat (20% of energy as fat), moderate cholesterol (0.1%, w/w) diet for 8 weeks in conjunction with biweekly injections (25 mg/kg) of saline, a non-targeting ASO (*control ASO*), or an ASO targeting the knockdown of ACAT2 (*ACAT2 ASO*). Mice with targeted gene deletion of ACAT2 were treated with saline as a total body knock-out control (*ACAT2*$^{-/-}$). Fasting liver samples were extracted and enzymatically analyzed to quantify the mass of: *A*, TC; *B*, CE; *C*, FC; and *D*, PL. All hepatic lipid values were normalized to the wet weight of the extracted tissue, and represent the mean ± S.E. from seven to nine mice per group. Values not sharing a common superscript differ significantly ($p < 0.05$).

perfusion, ACAT2 ASO-treated livers had augmented secretion rates of free cholesterol and phospholipid when compared with control ASO-treated or ACAT2$^{-/-}$ livers (Fig. 6*A*). Although significant differences were not detected, the previously reported trend toward increased TG secretion was seen for both ACAT2 ASO-treated and ACAT2$^{-/-}$ mice when compared with control ASO-treated mice (Fig. 6*A*).

Because ACAT2 ASO-treated livers secreted normal levels of CE during perfusion, we questioned whether the knockdown efficiency of ACAT2 was as complete as had been previously demonstrated in the set of livers used for perfusion (14) (Fig. 1, *B*, *D*, and *F*). Indeed, in the perfused livers from mice that had been treated for 8 weeks with the ACAT2 ASO, ACAT2 protein levels (Fig. 6*B*) and activity (data not shown) were dramatically (>99%) reduced. Therefore, the unexplained hepatic CE secretion seen during perfusion of ACAT2 ASO-treated livers may arise from residual ACAT2 activity or increased LCAT activity in the perfusate medium. To address these possibilities we examined LCAT activity in the final perfusate time point, and found it very low (<1% of LCAT activity found in normal mouse plasma; data not shown), which is in agreement with previous reports (20). Because LCAT activity was negligible in liver perfusate, we next attempted to examine the fatty acid composition of perfusate CE to confirm that the perfusate CE were indeed ACAT2-derived, because ACAT2 preferentially uses 18:1 and 16:0 as a fatty acid substrate (19). Our suspicion was confirmed when we found that the CE in ACAT2 ASO-treated liver perfusate contained on average 36% of total fatty acids as 18:1, and 27% of total fatty acids as 16:0, and these values were not significantly different from those in CE of control ASO-treated perfusate (data not shown).

In a final attempt to explain the paradoxical finding that the CE secretion rate was equivalent in ACAT2 ASO-treated liver, yet absent in ACAT2$^{-/-}$ livers after 8 weeks of treatment, we treated a subset of mice for an extended period of time (14–16 weeks) with ASOs with the hope of completely inhibiting ACAT2 expression with prolonged exposure. In this set of mice we also determined sterol secretion rates by gas-liquid chromatography rather than enzymatically to rule out misidentification of the sterols being secreted by the liver. The resulting chromatograms indicated that all sterol detected in liver perfusates was indeed cholesterol, without any detectable sterol intermediates (data not shown). Interestingly, after the more chronic ASO treatment, two of the four ACAT2 ASO-treated livers had no detectable CE secretion (Fig. 6*C*), and one showed abundant CE secretion. Importantly, in the two ACAT2 ASO-treated livers that lacked CE secretion, an augmentation of FC secretion was apparent (Fig. 6*C*, denoted by *arrows*). Collectively, these data suggest that even in the face of a 99.3% reduction of hepatic ACAT2 activity (8 weeks of ASO treatment, Fig. 1*F*), the remaining 0.7% of ACAT2 is sufficient to drive hepatic secretion of 18:1- and 16:0-enriched CE (Fig. 6*A*), but is not adequate to promote hepatic storage of CE (Fig. 3*B*). However, a longer term (14–16 weeks) ACAT2 ASO treatment prevented both hepatic CE storage and secretion (Fig. 6*C*) in some mice. This discrepancy may indicate that an almost 100% reduction in ACAT2 activity is needed to prevent CE secretion, whereas a more modest reduction is needed to reduce hepatic CE stores.

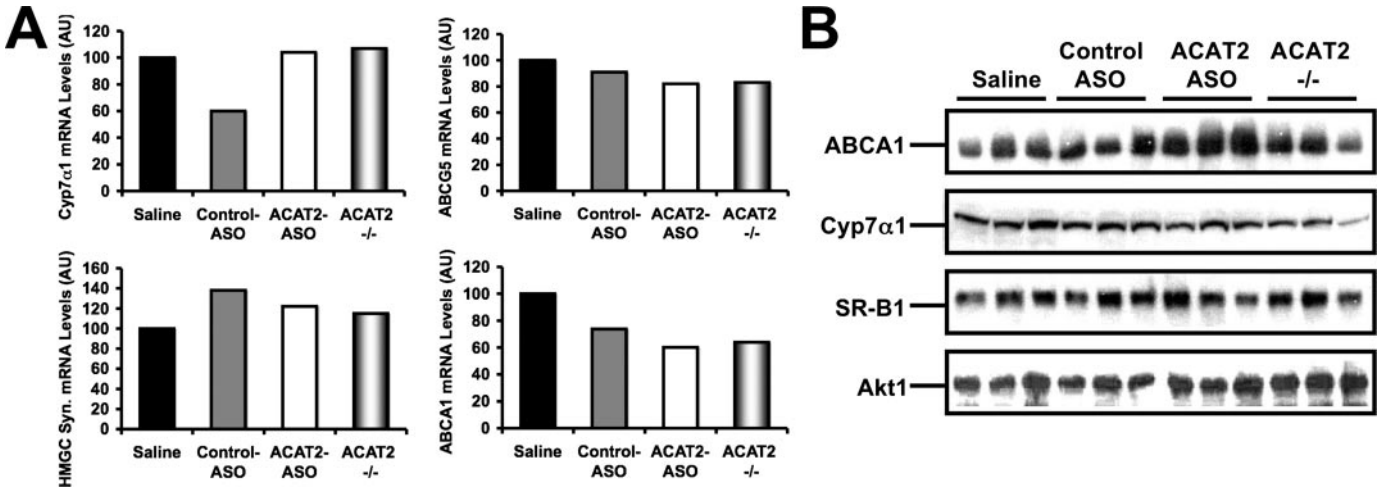

FIGURE 4. **The hepatic expression of cholesterol-sensitive genes.** *A*, the hepatic expression of ATP binding cassette transporter A1 (*ABCA1*), ATP binding cassette transporter A5 (*ABCG5*), 3-hydroxy-3-methylglutaryl-CoA synthase 1 (*HMGC syn.*), and Cyp7α1 were measured in pooled samples ($n = 5$) by quantitative PCR as described under "Experimental Procedures." *B*, the hepatic protein expression of ABCA1, Cyp7α1, scavenger receptor-BI (*SR-BI*), and Akt1 were measured by Western blotting in individual mice ($n = 3$ per group), as described under "Experimental Procedures."

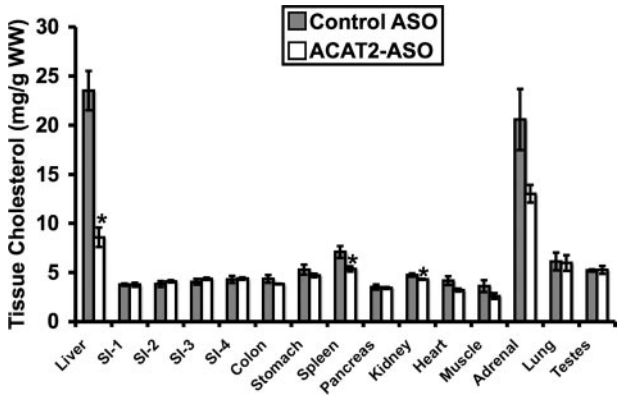

FIGURE 5. **ASO-mediated depletion of hepatic cholesterol esterification does not result in cholesterol accumulation in extrahepatic tissues.** Male LDLr$^{-/-}$, apoB100-only mice were fed a low-fat (20% of energy as fat), moderate cholesterol (0.1%, w/w) diet for 8 weeks in conjunction with biweekly injections (25 mg/kg) of either a non-targeting ASO (*control ASO*) or an ASO targeting the knockdown of ACAT2 (*ACAT2 ASO*). Thereafter, multiple tissues were extracted and analyzed to determine total cholesterol content of each tissue. All cholesterol mass values were normalized to the wet weight of the extracted tissue, and represent the mean ± S.E. from 4 mice per group. *Asterisk*, significantly different from the control ASO group within each lipid classification ($p < 0.05$). SI was segmented into 4 equal parts and is represented proximal to distal as SI-1, SI-2, SI-3, and SI-4.

We are currently attempting to address this paradox by creating liver-specific ACAT2 knock-out mice by gene targeting.

ASO-mediated Depletion of Hepatic ACAT2 Promotes Fecal Neutral Sterol Loss Without Altering Biliary Sterol Secretion—Because ACAT2 ASO treatment results in a liver-specific depletion of ACAT2 that leaves intestinal ACAT2 expression and cholesterol absorption intact (Fig. 1), there are abundant amounts of absorbed dietary cholesterol available to the liver and extrahepatic tissues for their metabolic needs. Strikingly, under these conditions (*i.e.* ACAT2 ASO treatment), with a moderate dietary cholesterol burden (0.1%, w/w), there is no accumulation of cholesterol in the plasma (Fig. 2) or in any tissue examined (Figs. 3 and 5). Therefore, we examined whether there were alterations in fecal loss of cholesterol that could help explain this discrepancy. Indeed, both ACAT2 ASO-treated mice and ACAT2$^{-/-}$ mice had a ~2-fold increase in fecal neutral sterol loss when compared with their respective control group (Fig. 7*A*).

Altered fecal sterol loss is typically reflective of hepatobiliary sterol excretion in the face of equivalent dietary cholesterol intake, so we examined the mass of neutral and acidic sterols in gall bladder bile (Fig. 7*B*). Surprisingly gall bladder bile samples exhibited no significant difference in cholesterol, bile acid, or PL concentrations among groups. Furthermore, when gall bladder bile data were expressed as % molar concentration, cholesterol concentration was significantly reduced in ACAT2$^{-/-}$ mice and although not different, trended toward a reduction in the ACAT2 ASO-treated groups compared with controls (Fig. 7*B*). This unexpected reduction in gall bladder bile cholesterol concentration as seen in ACAT2$^{-/-}$ mice is consistent with our previous findings (13). Because we could not reconcile the fact that ACAT2 depletion resulted in a 2-fold increase in fecal neutral sterol loss (Fig. 7*A*) without increasing the secretion of sterol in gall bladder bile (Fig. 7*B*), we performed common bile duct cannulations to collect newly secreted bile that had not undergone any concentration in the gall bladder.

As seen in Fig. 7*C*, the results for biliary sterol excretion into newly secreted bile were similar to those seen with gall bladder bile. In newly secreted bile, ACAT2$^{-/-}$ had significantly lower concentrations (μmol/ml) of biliary cholesterol (Fig. 7*C*), when compared with all other groups. However, in newly secreted bile, there were no significant alterations in cholesterol, bile acid, or PL in mice treated with the ACAT2 ASO. Collectively, these data suggest that hepatic ACAT2 depletion (either through ASO treatment or gene deletion) results in a 2-fold increase in fecal neutral sterol output, yet results in either decreased (in the case of ACAT2$^{-/-}$ mice) or normal (in the case of ACAT2 ASO treatment) hepatobiliary sterol excretion.

ASO-mediated Depletion of Hepatic ACAT2 Promotes Non-biliary (Liver → Plasma → Small Intestine → Feces) Fecal Loss—We believe in order to reconcile the disconnect between biliary sterol excretion and fecal sterol loss, a non-biliary route of fecal neutral sterol loss must exist in conditions where hepatic cho-

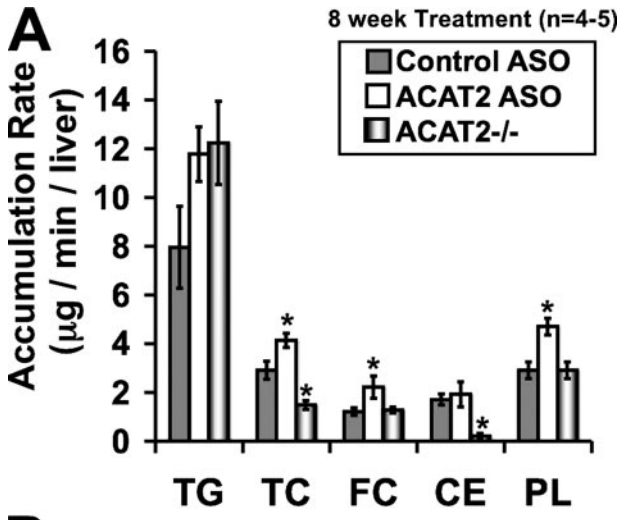

C

Sterol Secretion Rate (μg/min/g liver) After 14-16 Week TRT

Treament Group	Free Cholesterol	Cholesterol Ester
Control ASO	1.08	1.38
Control ASO	0.92	1.31
Control ASO	1.74	0.22
Control ASO	1.69	0.54
ACAT2 ASO	0.71	1.26
ACAT2 ASO	3.82	0 ←
ACAT2 ASO	5.03	0 ←
ACAT2 ASO	1.89	0.29

FIGURE 6. **Depletion of hepatic ACAT2 results in augmented free cholesterol and phospholipid secretion during isolated liver perfusion.** Male LDLr$^{-/-}$, apoB100-only mice were fed a low-fat (20% of energy as fat), moderate cholesterol (0.1%, w/w) diet for 8 weeks (*A* and *B*) or 14–16 weeks (*C*) in conjunction with biweekly injections (25 mg/kg) of a non-targeting ASO (*control ASO*) or an ASO targeting the knockdown of ACAT2 (*ACAT2 ASO*). Mice with targeted gene deletion of ACAT2 were treated with saline for 8 weeks as a total body knock-out control (*ACAT2*$^{-/-}$). Thereafter, isolated liver perfusions were carried out to determine the mass accumulation rates of TG, TC, CE, FC, and PL. Data in *panel A* represent the mean ± S.E. from 5 control ASO-treated mice, 5 ACAT2 ASO-treated mice, and 4 ACAT2$^{-/-}$ mice; *asterisk*, significantly different from the control ASO group within each lipid classification ($p < 0.05$). *Panel B* represents Western blot confirmation that ACAT2 protein was not detectable in the ACAT2 ASO-treated or ACAT2$^{-/-}$ livers used for perfusion following 8 weeks of treatment. *NS*, nonspecific background band that serves as a loading control. *Panel C* represents a subset of mice that were chronically (14–16 weeks) treated with ASOs. Lipid accumulation rates in *panel C* were determined by gas-liquid chromatography.

lesterol esterification is limited (*i.e.* ACAT2 ASO treatment). To test this hypothesis we devised a protocol designed to track the fate of newly secreted liver-derived cholesterol once it reaches the plasma compartment (Fig. 8*A*). To this end we radiolabeled hepatic sterol pools with [^{3}H]cholesterol, and utilized isolated liver perfusion to collect nascent hepatic [^{3}H]cholesterol-labeled lipoproteins from ASO-treated mice. These liver-derived lipoproteins were then re-injected intravenously into ASO-treated recipient mice to examine movement of this liver-derived [^{3}H]cholesterol source into the lumen of the small intestine. As seen in Fig. 8*B*, the movement of liver-derived [^{3}H]cholesterol from the plasma back to the liver and into bile was not significantly different between control and ACAT2 ASO-treated recipient mice. However, when [^{3}H]cholesterol-labeled perfusate from an ACAT2 ASO donor was reinjected into either a control ASO- or ACAT2 ASO-treated recipient, there was preferential trafficking of this cholesterol into the wall and lumen of the most proximal segment (SI-1) of the small intestine (Fig. 8*B*). In fact, there was a 3.3- and 2.1-fold increase in SI-1 lumenal contents and SI-1 intestinal wall recovery, respectively, when comparing the ACAT2 ASO-donor ⋙ ACAT2 ASO recipient group to the control ASO-donor ⋙ control ASO recipient group. Interestingly, in all groups the amount of [^{3}H]cholesterol found in the small intestine wall and lumenal contents was much higher in the proximal segments (SI-1 and SI-2), when compared with distal segments (SI-3 and SI-4), supporting a proximal to distal gradient of [^{3}H]cholesterol recovery.

DISCUSSION

It has long been understood that the liver plays a central role in maintaining whole body cholesterol homeostasis by elegantly balancing *de novo* synthesis, uptake from plasma lipoproteins, input from intestinal absorption, biliary secretion, and packaging for secretion in nascent lipoproteins (1–5). It has been the prevailing thought that hepatic ACAT2 likely plays a gatekeeper role in this balancing act, and that alterations in hepatic ACAT2 activity would likely impact all of these homeostatic mechanisms. The current study provides unexpected insight into the hepatic itinerary of cholesterol under conditions where it cannot readily be esterified by ACAT2. Under such limiting conditions we have been able to demonstrate that: 1) cholesterol levels on apoB-containing lipoproteins are reduced without altering HDL cholesterol, 2) hepatic CE storage is strongly reduced without reciprocal accumulation of hepatic FC, 3) the hepatic secretion of FC is increased while CE secretion is normal or low, 4) fecal sterol loss is increased in the absence of changes in biliary sterol excretion, and 5) newly secreted liver-derived cholesterol is preferentially shunted to the proximal small intestine for basolateral to apical excretion. The finding that ACAT2 ASO treatment results in diminished hepatic cholesterol storage and limited packaging into apoB-containing lipoprotein is consistent with previous results (9–16). However, the fact that fecal sterol loss is increased without changes in biliary sterol excretion is quite perplexing, and may represent a novel non-biliary pathway for fecal sterol loss that warrants further examination.

Using ASO-mediated knockdown of ACAT2 we have been able to create a situation where abundant dietary cholesterol can reach the liver, but once taken up by the liver cannot be esterified. This resulted in striking reduction of stored cholesterol ester in the liver, yet did not result in reciprocal accumulation of hepatic free cholesterol. This discrepancy is not likely explained by compensatory transcriptional alterations in *de novo* sterol synthesis or sterol efflux onto nascent HDL, because both SREBP2- and LXR-target genes as well as HDL-C levels were not altered by ACAT2 ASO treatment, findings in agree-

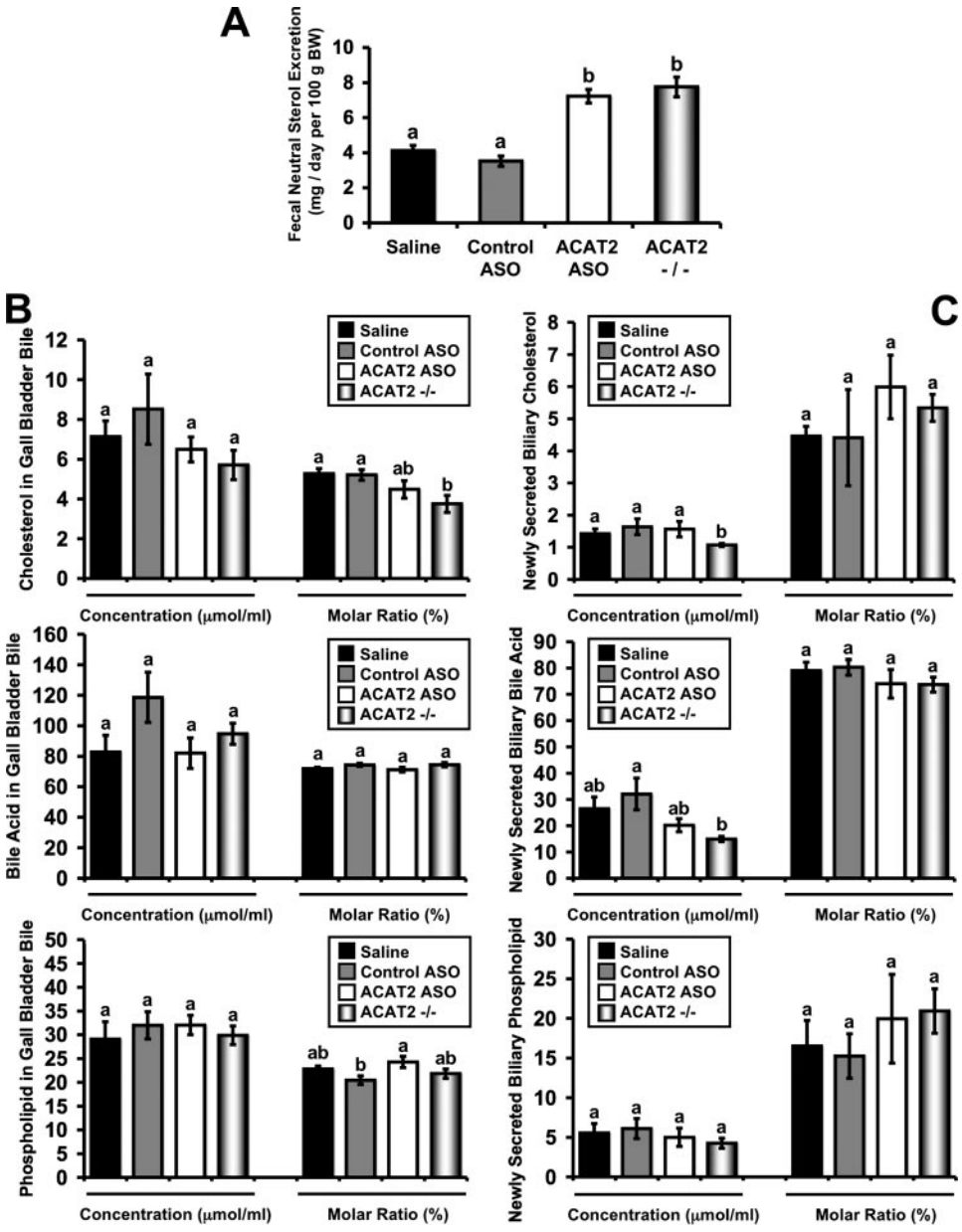

FIGURE 7. **ASO-mediated depletion of hepatic ACAT2 promotes fecal neutral sterol excretion without altering biliary sterol secretion.** Male LDLr$^{-/-}$, apoB100-only mice were fed a low-fat (20% of energy as fat), moderate cholesterol (0.1%, w/w) diet for 8 weeks in conjunction with biweekly injections (25 mg/kg) of saline, a non-targeting ASO (*control ASO*), or an ASO targeting the knockdown of ACAT2 (*ACAT2 ASO*). Mice with targeted gene deletion of ACAT2 were treated with saline as a total body knock-out control (*ACAT2*$^{-/-}$). *A*, feces were collected for 3 days and the mass amount of fecal neutral sterol was determined by gas-liquid chromatography. Data shown in *panel A* represent the mean ± S.E. from seven to nine mice per group, and values not sharing a common superscript differ significantly ($p < 0.05$). *B*, cholesterol, bile acid, and phospholipid concentrations in gall bladder bile. Data shown in *panel B* represent the mean ± S.E. from six to seven mice per group, and values not sharing a common *superscript* differ significantly ($p < 0.05$). *C*, newly secreted biliary cholesterol, bile acid, and phospholipid concentrations following common bile duct cannulation collections. Data shown in *panel C* represent the mean ± S.E. from four to six mice per group, and values not sharing a common *superscript* differ significantly ($p < 0.05$).

ment with results in ACAT2$^{-/-}$ mice (12, 13). Furthermore, this lack of free cholesterol build up also cannot be reconciled by increased hepatobiliary neutral or acidic sterol output. These findings are in agreement with elegant studies done by Turley and Dietschy (23) that clearly demonstrated in rats that the level of hepatic cholesteryl ester (which were varied over 100-fold in this study) had no impact on the rate of biliary cholesterol secretion. So the question remains: how does the liver deal with the excess dietary free cholesterol burden when hepatic ACAT2 cannot readily detoxify it by esterification?

One possible explanation could lie in the fact that ACAT2 ASO-treated liver secretes more free cholesterol into the plasma compartment during isolated liver perfusion (Fig. 4). It remains possible that under conditions where hepatic cholesterol esterification is limited (*i.e.* ACAT2 ASO treatment), the liver does not deal with the cholesterol burden using the traditional mechanisms of repression of *de novo* cholesterol synthesis, increasing biliary secretion, conversion to bile acid, or efflux onto nascent HDL. Instead, our data support a model where none of these traditional pathways are utilized, and the unesterified cholesterol seems to exit the liver directly into the plasma compartment during isolated liver perfusion. Intriguingly, this liver-derived cholesterol seems to be preferentially shunted to the proximal small intestine for direct basolateral to apical secretion through an ill-defined process that is separate from biliary cholesterol output.

Almost five decades ago it was first suggested that non-dietary fecal sterol loss in humans consists of two distinct fractions: 1) the traditional fraction coming from hepatobiliary secretion, and 2) an elusive fraction directly secreted by the intestine (24). Fourteen years later experiments utilizing complete biliary diversion in dogs fed a cholesterol-free diet provided additional evidence for a non-biliary route of neutral sterol loss (25). This study demonstrated that biliary diversion resulted in complete loss of fecal acidic sterol output, yet fecal neutral sterol output actually increased (25). Based on this observation, the authors speculated "the increased output of fecal neutral steroids could be the result of transfer of plasma cholesterol across the gut wall or due to increased synthesis in the gut." These early speculations were largely ignored because they did not agree with the dogma that fecal sterol loss occurs exclusively as a result of biliary secretion. However, evidence for non-bilary fecal sterol loss continues to come to light in the age of genetically modified mice.

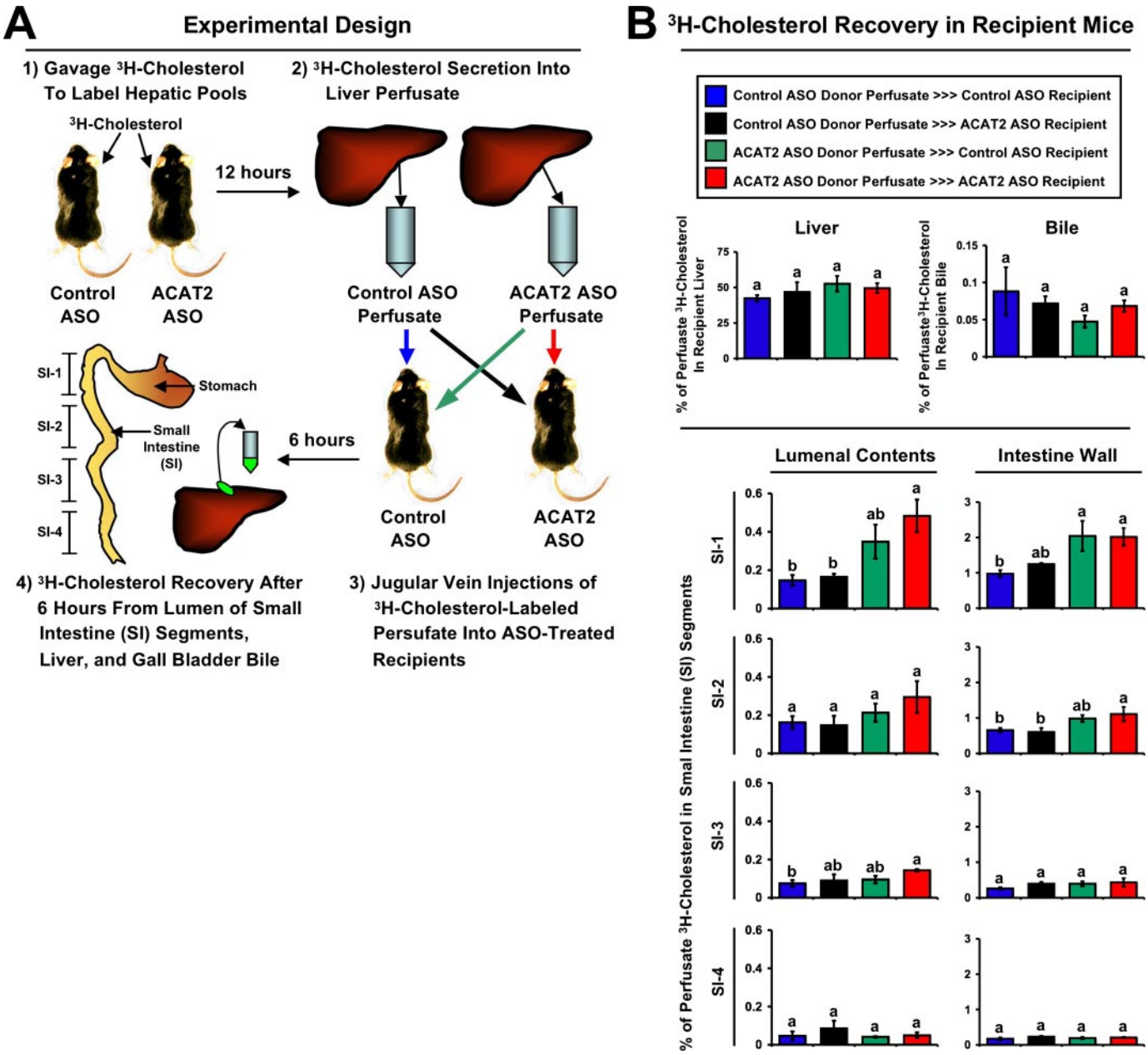

FIGURE 8. **ASO-mediated depletion of hepatic ACAT2 promotes non-biliary intestinal secretion of cholesterol.** *A* represents the experimental design for this study. Briefly, control ASO and ACAT2 ASO-treated mice ($n = 3$ donor mice per group) were gavaged with 50 μCi of [^{3}H]cholesterol, and 12 h later isolated liver perfusions were done to collect perfusate samples that contained newly secreted liver-derived lipoprotein-associated [^{3}H]cholesterol. Aliquots of [^{3}H]cholesterol-labeled perfusate were introduced intravenously into recipient mice that had been treated with either a control ASO or ACAT2 ASO. Six hours later, gall bladder bile, liver, SI lumenal contents, and small intestine wall were collected to determine [^{3}H]cholesterol recovery. The SI was segmented into 4 equal parts and is represented proximal to distal as SI-1, SI-2, SI-3, and SI-4. *B* represents the [^{3}H]cholesterol recovery in recipient mice, and the *colored bars* should be referenced to donor-recipient crossover design that is represented by *similar colored arrows* in *A*. All data in *B* are expressed as a percentage (%) of the original injected [^{3}H]cholesterol-labeled perfusate dose recovered in each tissue compartment. Bile data is represented as the % of [^{3}H]cholesterol-labeled perfusate dose found in 10 μl of gall bladder bile. Data shown represent the mean ± S.E. from three to four recipient mice per group, and values not sharing a common superscript differ significantly ($p < 0.05$).

Our model now represents the fourth known mouse model that shows increased neutral sterol loss without parallel changes in biliary sterol excretion (17, 26, 27), supporting the presence of a similar non-biliary route for fecal sterol excretion in murine models. The first mouse model described with this discrepancy was the cholesterol 7α-hydroxylase-deficient mouse (26). In these mice, fecal sterol loss was double that of wild type controls, with no apparent change in biliary sterol output (26). In further support of this concept, Kruit *et al.* (27) examined LXR agonist-activated increases in fecal sterol loss in a mouse model that lacks biliary cholesterol secretion (Mdr2$^{-/-}$). This study was a powerful demonstration that in a mouse where biliary sterol secretion is non-functional, LXR activation still resulted in large increases in fecal sterol output, supporting the presence of an LXR-inducible non-biliary pathway for fecal sterol loss (27). Furthermore, our group has recently created a model where Niemann-Pick C1-like 1 (NPC1L1) was overexpressed in mouse liver to examine the role of this protein in

biliary sterol transport (17). Strikingly, hepatic NPC1L1 overexpression resulted in >90% reduction of biliary cholesterol levels, yet fecal sterol output remained similar to wild type mice (17).[3] Probably not coincidentally, all of these mouse models are conditions where free cholesterol could potentially build up locally in the liver due to defects in normal elimination pathways. It remains possible that under conditions where hepatic free cholesterol burden becomes too excessive for disposal through biliary secretion (*i.e.* ACAT2 ASO treatment, Cyp7$\alpha^{-/-}$ mice (26), Mdr2$^{-/-}$ mice (27), or liver-specific NPC1L1 transgenic mice (17)), an alternative plasma-based route of fecal disposal exists that has yet to be clearly defined.

In fact, the non-biliary route of fecal sterol loss may play a substantial role in maintaining sterol balance, making up a large portion of fecal neutral sterol excretion in both mice (28) and man (29). To address the quantifiable importance of this pathway in mice, Plosch and colleagues (28) treated wild type and ABCA1-deficient mice with the synthetic LXR agonist T0901317 and quantified amounts dietary cholesterol, biliary cholesterol, and fecal cholesterol to get an estimate of this non-biliary pathway. Results from this study suggested that ~36% of the total fecal cholesterol loss could be attributed to the non-biliary intestinal secretion pathway, demonstrating that this pathway represents an important LXR-inducible pathway for mass fecal sterol loss in mice (28). One attempt to quantify the importance of this pathway in humans was conducted by Simmonds and colleagues (29) using an intestinal perfusion system. Using micellar radiolabeled cholesterol and calculating specific activity changes, the authors concluded: "cholesterol was absorbed by, and in all probability, secreted by the test segment." This study estimated that ~44% of total fecal sterol output in the perfused intestinal test segment originated from endogenous sources (29). Most recently, Van der Velde and colleagues (30) using a mouse intestinal perfusion system demonstrated that plasma cholesterol can traverse the small intestine in a basolateral to apical direction in a process that is dependent on bile salt and phospholipid acceptors being present in the intestinal lumen (30). Intriguingly, these authors reported that transintestinal cholesterol secretion occurs most readily in the proximal 10 cm of the small intestine, a result similar to our findings (Fig. 8*B*). Collectively, these data support the idea that fecal sterol loss is a mixture of dietary, biliary, and intestinally derived sterol; the origins of the latter source have yet to be elucidated.

In the original report describing the phenotypic characterization of ACAT2$^{-/-}$ mice, Buhman and colleagues (11) reported that ACAT2 deficiency conferred quantitative resistance to gallstone formation in mice fed a lithogenic diet. These investigators did not investigate biliary sterol levels, but speculated that most of this protective effect was due to diminished cholesterol absorption in the intestine, which would provide less hepatic substrate for lithogenic bile formation. However, an earlier study demonstrated that hepatic ACAT activity was lower in gallstone patients when compared with controls, and speculated that diminished hepatic ACAT activity may allow for more free cholesterol secretion into bile in humans (31). Our results argue against the latter possibility, because ACAT2$^{-/-}$ mice, which completely lack hepatic cholesterol esterification, actually have significantly less free cholesterol in gall bladder bile (13) (Fig. 7*B*) or newly secreted bile (Fig. 7*C*) compared with controls. Collectively, our data suggest that Buhman and colleagues (11) were correct in their assumption that the protection against gallstone formation seen in ACAT2$^{-/-}$ mice is related to diminished intestinal cholesterol absorption thereby limiting hepatic cholesterol availability.

In addition to the paradoxical disconnect between fecal and biliary sterol excretion in ACAT2 ASO-treated mice, we found an equally perplexing outcome in that hepatic secretion of CE was normal in ACAT2 ASO-treated mice during isolated liver perfusion (Fig. 6*A*). We originally thought that the knockdown of ACAT2 was incomplete in those livers, but Western blotting confirmed that ACAT2 ASO-treated livers had almost no detectable (<1% of control ASO-treated levels) ACAT2 protein (Fig. 6*B*). Furthermore, the CE found in ACAT2 ASO-treated liver perfusate contained the signature of ACAT2-derived CE (enriched in 18:1 and 16:0), whereas LCAT activity was negligible in those samples (data not shown). Based on these findings it is possible that only a small amount (<1% of normal) of ACAT2 is needed to drive the packaging of hepatic CE into apoB-containing lipoproteins. More work is needed to strengthen this speculation but it is interesting to wonder whether this finding suggests that the secretion of CE in VLDL that normally occurs from the liver requires only a small fraction of hepatic ACAT2. This information may be important because the relative abundance of ACAT2 protein in human liver is much lower than levels found in mouse liver (7, 32), yet the small amount present may be sufficient to support packaging of CE into atherogenic apoB-containing lipoproteins in humans.

In conclusion, the results from this study once again underscore the importance of hepatic ACAT2-driven cholesterol esterification in promoting the production of atherogenic apoB-containing lipoproteins, and shed new light into the role of hepatic ACAT2 in regulating non-biliary fecal sterol loss. Importantly, if ACAT2-specific inhibitors could be developed for use in humans, they would work in parallel to statins through distinct mechanisms to lower LDL cholesterol by preventing VLDL cholesterol packaging and promoting fecal sterol loss through a novel non-biliary pathway. Studies to identify the proteins involved and the itinerary of cholesterol through this poorly defined non-biliary "liver > plasma > proximal small intestine > feces" pathway are currently underway.

[3] J. M. Brown, R. E. Temel, L. Yu, and L. L. Rudel, unpublished observations.

REFERENCES

1. Dietschy, J. M., and Turley, S. D. (2002) *J. Biol. Chem.* **277,** 3801–3804
2. Dietschy, J. M., Turley, S. D., and Spady, D. K. (1993) *J. Lipid Res.* **34,** 1637–1659
3. Horton, J. D., Goldstein, J. L., and Brown, M. S. (2002) *J. Clin. Investig.* **109,** 1125–1131
4. Brown, M. S., Kovanen, P. T., and Goldstein, J. L. (1981) *Science* **212,** 628–635
5. Turley, S. D., and Dietshcy, J. M. (2003) *Curr. Opin. Lipidol.* **14,** 233–240
6. Rudel, L. L., Lee, R. G., and Parini, P. (2005) *Arterioscler. Thromb. Vasc. Biol.* **25,** 1112–1118
7. Parini, P., Davis, M. A., Lada, A. T., Erickson, S. K., Wright, T. L., Gustafs-

son, U., Sahlin, S., Einarsson, C., Erickson, M., Angelin, B., Tomoda, H., Omura, S., Willingham, M. C., and Rudel, L. L. (2004) *Circulation* **110,** 2017–2023
8. Lee, R. G., Willingham, M. C., Davis, M. A., Skinner, K. A., and Rudel, L. L. (2000) *J. Lipid Res.* **41,** 1991–2001
9. Lee, R. G., Shah, R., Sawyer, J. K., Hamilton, R. L., Parks, J. S., and Rudel, L. L. (2005) *J. Lipid Res.* **46,** 1205–1212
10. Lee, R. G., Kelley, K., Sawyer, J., Farese, R. V., Parks, J. S., and Rudel, L. L. (2004) *Circ. Res.* **95,** 998–1004
11. Buhman, K., Accad, M., Novak, S., Choi, R., Wong, J., Hamilton, R., Turley, S., and Farese, R. (2000) *Nat. Med.* **6,** 1341–1347
12. Repa, J. J., Buhman, K., Farese, R., Dietschy, J., and Turley, S. (2004) *Hepatology* **40,** 1088–1097
13. Temel, R. E., Lee, R. G., Kelley, K. L., Davis, M. A., Shah, R., Sawyer, J. K., Wilson, M. D., and Rudel, L. L. (2005) *J. Lipid Res.* **46,** 2423–2431
14. Bell, T. A., III, Brown, J. M., Graham, M. J., Lemonidis, K. M., Crooke, R. M., and Rudel, L. L. (2006) *Arterioscler. Thromb. Vasc. Biol.* **26,** 1814–1820
15. Willner, E., Tow, B., Buhman, K., Wilson, M., Sanan, D., Rudel, L. L., and Farese, R. (2003) *Proc. Natl. Acad. Sci. U. S. A.* **100,** 1262–1267
16. Bell, T. A., III, Kelley, K., Wilson, M. D., Sawyer, J. K., and Rudel, L. L. (2007) *Arterioscler. Thromb. Vasc. Biol.* **27,** 1396–1402
17. Temel, R. E., Tang, W., Ma, Y., Rudel, L. L., Willingham, M. C., Ioannou, Y. A., Davies, J. P., Nilsson, L. M., and Yu, L. (2007) *J. Clin. Investig.* **117,** 1968–1978
18. Dawson, P. A., Haywood, J., Craddock, A. L., Wilson, M., Tietjen, M., Kluckman, K., Maeda, N., and Parks, J. S. (2003) *J. Biol. Chem.* **278,** 33920–33927
19. Rudel, L. L., Haines, J., Sawyer, J. K., Shah, R., Wilson, M. S., and Carr, T. P. (1997) *J. Clin. Investig.* **100,** 74–83
20. Johnson, F. L., St. Clair, R. W., and Rudel, L. L. (1986) *J. Clin. Investig.* **72,** 221–236
21. Bligh, E. G., and Dyer, W. J. (1959) *Can. J. Biochem. Physiol.* **37,** 911–917
22. Butler, M., Stecker, K., and Bennett, C. F. (1997) *Lab. Investig.* **77,** 379–388
23. Turley, S. D., and Dietschy, J. M. (1979) *J. Lipid Res.* **20,** 923–934
24. Cheng, S. H., and Stanley, M. M. (1959) *Proc. Soc. Exp. Biol. Med.* **101,** 223–225
25. Pertsemlidis, D., Kirchman, E. H., and Ahrens, E. H., Jr. (1973) *J. Clin. Invest.* **52,** 2353–2367
26. Schwarz, M., Russell, D. W., Dietschy, J. M., and Turley, S. D. (1998) *J. Lipid Res.* **39,** 1833–1843
27. Kruit, J. K., Plosch, R., Havinga, R., Boverhof, R., Groot, P. H., Groen, A. K., and Kuipers, F. (2005) *Gastroenterology* **128,** 147–156
28. Plosch, T., Kok, T., Bloks, V. W., Smit, M. J., Havinga, R., Chimini, G., Groen, A. K., and Kuipers, F. (2002) *J. Biol. Chem.* **277,** 33870–33877
29. Simmonds, W. J., Hofmann, A. F., and Theodor, E. (1967) *J. Clin. Investig.* **46,** 874–890
30. Van der Velde, A. E., Vrins, C. L., van den Oever, K., Kunne, C., Oude Elferink, R. P., Kuipers, F., and Groen, A. K. (2007) *Gastroenterology* **133,** 967–975
31. Smith, J. L., Hardie, I. R., Pillay, S. P., and de Jersey, J. (1990) *J. Lipid Res.* **31,** 1993–2000
32. Chang, C. C., Sakashita, N., Ornvold, K., Lee, O., Chang, E. T., Dong, R., Lin, S., Lee, C. Y., Strom, S. C., Kashyap, R., Fung, J. J., Farese, R. V., Jr., Patoiseau, J. F., Delhon, A., and Chang, T. Y. (2000) *J. Biol. Chem.* **275,** 28083–28092